Journal of Engineering Physics and Thermophysics, Vol. 80, No. 4, 2007

INTERPHASE MASS TRANSFER BETWEEN LIQUID–LIQUID COUNTER-CURRENT FLOWS. II. MASS TRANSFER KINETICS

E. Horvath[a], E. Nagy[a], C. Boyadjiev[b], and J. Gyenis[a]

UDC 532.529.5

A theoretical analysis of mass-transfer kinetics based on the method of similarity variables for a liquid–liquid counter-current flow has been made. The numerical results obtained for the mass-transfer rate (Sherwood number) in the case of a laminar boundary layer with a flat interphase are compared with analogous results for a co-current flow. The ratio between the mass-transfer rate and the energy dissipation in the boundary layer is determined. The advantages of the co-current flow due to lower energy losses compared with the case of the counter-current one are shown.

Introduction. In our previous work, the velocity distribution in a laminar boundary layer of a liquid–liquid counter-current flow with a flat interphase was determined [1]. The results obtained allowed us to determine energy dissipation in the boundary layer and to compare this with the corresponding value in the case of a co-current flow. The subject of the present work is the comparison of the mass-transfer kinetics and the ratio between the mass-transfer rate and energy dissipation for co- and counter-current flows of two immiscible liquids in which a certain substance is dissolved.

Mathematical Model. The mass-transfer rate is determined by solution of the convection-diffusion equation. The boundary conditions at the interphase are formulated for the case of mass transfer between two liquids [2] with account for the thermodynamic equilibrium and the continuity of the mass flux. In this way, the mathematical model of the interphase mass transfer in liquid–liquid systems with a counter-current flow in a laminar boundary layer with a flat interphase takes the following form:

$$u_i \frac{\partial c_i}{\partial x} + v_i \frac{\partial c_i}{\partial y} = D_i \frac{\partial^2 u_i}{\partial y^2}, \quad i = 1, 2;$$

$$x = 0, \quad y \geq 0, \quad c_1 = c_1^{\infty};$$

$$x = l, \quad y \leq 0, \quad c_2 = c_2^{\infty};$$

$$y \to \infty, \quad 0 \leq x \leq l, \quad c_1 = c_1^{\infty}; \tag{1}$$

$$y \to -\infty, \quad 0 \leq x \leq l, \quad c_2 = c_2^{\infty};$$

$$y = 0, \quad 0 < x < l, \quad c_1 = \chi c_2, \quad D_1 \frac{\partial c_1}{\partial y} = D_2 \frac{\partial c_2}{\partial y},$$

where the velocity components in the liquids u_i and v_i were obtained in [1] and c_i^{∞} is the input concentration of the transferred substance.

[a]University of Veszprém, Research Institute Chemical Process Engineering, 8201 Veszprém, P.O.B. 125, Hungary; [b]Bulgarian Academy of Sciences, Institute of Chemical Engineering, 1113 Sofia, Acad. G. Bontchev Str., Bl. 103, Bulgaria. Published in Inzhenerno-Fizicheskii Zhurnal, Vol. 80, No. 4, pp. 86–90, July–August, 2007. Original article submitted January 26, 2006; revision submitted June 20, 2006.

Method of Solution. For solution of problem (1), the following dimensionless variables and parameters will be used:

$$x = lX_1 = l - lX_2\,, \quad y = \delta_1 Y_1 = -\delta_2 Y_2\,, \quad \delta_i = \sqrt{\frac{\nu_i l}{u_i^{\infty}}}\,,$$

$$\varphi_i = (-1)^i \frac{c_i^{\infty} - c_i}{c_1^{\infty} - \chi c_2^{\infty}} \chi^{i-1}\,, \quad \varphi_i = \varphi_i(\eta_i)\,, \quad \eta_i = \frac{Y_i}{\sqrt{X_i}} = (-1)^{i+1} y \sqrt{\frac{u_i^{\infty}}{\nu_i l X_i}}\,,$$

$$\theta_2 = \left(\frac{\rho_1\mu_1}{\rho_2\mu_2}\right)^{1/2} \left(\frac{u_1^{\infty}}{u_2^{\infty}}\right)^{3/2}\,, \quad \bar{\theta}_2 = \theta_2 \sqrt{\frac{X_2}{X_1}}\,, \tag{2}$$

$$\theta_3 = \chi \frac{D_1}{D_2} \sqrt{\frac{u_1^{\infty}\nu_2}{u_2^{\infty}\nu_1}}\,, \quad \bar{\theta}_3 = \theta_3 \sqrt{\frac{X_2}{X_1}} = \theta_3 \sqrt{\frac{1 - X_1}{X_1}}\,.$$

As a result, problem (1) in the similarity variables (2) has the form

$$2\varphi_i'' + \mathrm{Sc}_i f_i \varphi_i' = 0\,, \quad \mathrm{Sc}_i = \frac{\nu_i}{D_i}\,,$$
$$\varphi_1(0) - \varphi_2(0) = 1\,, \quad -\bar{\theta}_3 \varphi_1'(0) = \varphi_2'(0)\,, \tag{3}$$

where f_i (i = 1, 2) are the solutions of Eq. (8) in [1]. It is clearly seen from Eq. (3) that it is possible to obtain the similarity solution for different values of $X_1 = 1 - X_2$. For this purpose, the values of X_1 are taken within the interval (0, 1). The system is investigated for $\theta_1 = 0.7$, $\theta_2 = 1.2$, $\mathrm{Sc}_1 = 812$, $\mathrm{Sc} = 440$, and $\theta_3 = 0.8029$ (see [1]).

The solution of differential equations (3) will be obtained under new boundary conditions for φ_i:

$$\varphi_1(0) = \alpha\,, \quad \varphi_1'(0) = \beta\,, \quad \varphi_2(0) = 1 - \alpha\,, \quad \varphi_2'(0) = -\bar{\theta}_3 \beta\,, \tag{4}$$

where α and β are determined for different values of X_1, so that the conditions $\lim_{\eta_i \to \infty} \varphi_i(\eta_i)$ are fulfilled.

Numerical Results. The numerical results can be obtained for interphase mass transfer of the substance with moderate solubility, i.e., for commensurable diffusion resistances ($\theta_3 = \chi \frac{D_1}{D_2} \frac{\mu_2}{\mu_1} \theta_1\theta_2 = 0.9558 \cdot 0.7 \cdot 1.2 = 0.8029$). We model interphase mass transfer of acetic acid between water (phase 1) and tetrachlorinemethane (phase 2) at 20°C. The system of differential equations should be solved after introducing the boundary conditions for different values of X_1.

The numerical results show (Fig. 1 and Table. 1) that the thicknesses of diffusion (concentration) boundary-layers are much less than those for laminar boundary layers (velocity layers). When the concentration boundary-layer line is between the interphase of the contact of two phases and the zero-velocity line (where the velocity is zero), different dimensionless convection-diffusion equations should be used (the velocity does not change direction in the concentration boundary-layers). Therefore, the system should be divided into three parts along the length. Two of them are the areas where the zero-velocity line is above ($0 < X_1 < X_0$) and below ($X_0 < X_1 < 1$) the concentration boundary-layer lines, and the third one is in the vicinity of the point where the zero-velocity line intersects the X axis. In these three areas, the corresponding convection-diffusion equations differ, i.e.,

$$2\varphi_i'' + (-1)^{\xi} \mathrm{Sc}_i f_i \varphi_i' = 0\,, \tag{5}$$

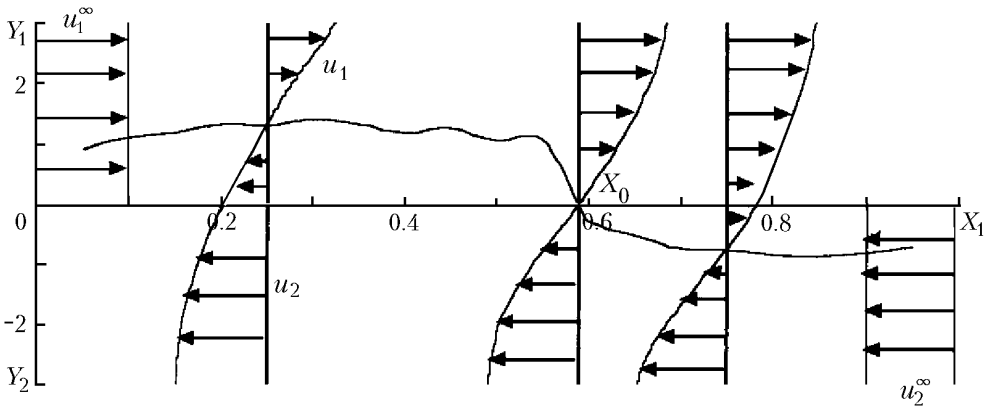

Fig. 1. Zero-velocity line and velocity distribution based on numerical calculations at $\theta_1 = 0.7$ and $\theta_2 = 1.2$.

TABLE 1. Numerical Results Obtained at $\theta_1 = 0.7$, $\theta_2 = 1.2$, $Sc_1 = 812$, $Sc_2 = 440$, and $\theta_3 = 0.8029$

X_1	$\varphi_1(0)$	$\varphi_1(1)$	$-\varphi_1'(0)$	Y_1^∞	Y_2^∞	$-\varphi_2(0)$	$\varphi_2(1)$	$\varphi_2'(0)$
0.05	0.2085	0.0059	1.7327	0.05	0.26	0.7915	0.0030	6.0638
0.10	0.2759	0.0067	2.4041	0.07	0.24	0.7241	0.0017	5.7906
0.15	0.3182	0.0005	2.9124	0.07	0.23	0.6818	0.0027	5.5662
0.20	0.3578	0.0011	3.3085	0.09	0.22	0.6422	0.0037	5.3126
0.25	0.3903	0.0001	3.6561	0.10	0.22	0.6097	0.0048	5.0842
0.30	0.4223	0.0005	3.9884	0.11	0.19	0.5777	0.0002	4.8914
0.35	0.4488	0.0001	4.2468	0.12	0.19	0.5512	0.0045	4.6466
0.40	0.4756	0.0007	4.4973	0.13	0.19	0.5244	0.0048	4.4223
0.45	0.5006	0.0001	4.7183	0.14	0.18	0.4994	0.0058	4.1880
0.50	0.5274	0.0000	4.9105	0.15	0.16	0.4726	0.0033	3.9425
0.55	0.5500	0.0003	4.9816	0.16	0.21	0.4500	0.0095	3.6178
0.5902	0.5427	0.0001	1.7345	0.36	0.37	0.4573	0.0009	1.1605
0.60	0.4903	0.0025	2.7213	0.24	0.55	0.5097	0.0008	1.7839
0.65	0.5748	0.0049	4.1799	0.20	0.20	0.4252	0.0010	2.4626
0.70	0.6083	0.0057	4.7648	0.19	0.16	0.3917	0.0004	2.5044
0.75	0.6418	0.0044	5.2032	0.19	0.13	0.3582	0.0010	2.4119
0.80	0.6807	0.0068	5.6408	0.19	0.10	0.3193	0.0095	2.2644
0.85	0.7131	0.0020	5.8674	0.23	0.10	0.2869	0.0021	1.9789
0.90	0.7715	0.0075	6.3825	0.22	0.06	0.2285	0.0186	1.7081
0.95	0.8206	0.0031	6.5044	0.26	0.05	0.1794	0.0008	1.1981
0.9999	0.9864	0.0001	5.4190	0.34	0.01	0.0136	0.0035	0.0435

where

$$\xi = i \quad \text{as} \quad 0 < X_1 < X_0 ,$$

$$\xi = i + 1 \quad \text{as} \quad X_1 = X_0 ,$$

$$\xi = 0 \quad \text{as} \quad X_0 < X_1 < 1 .$$

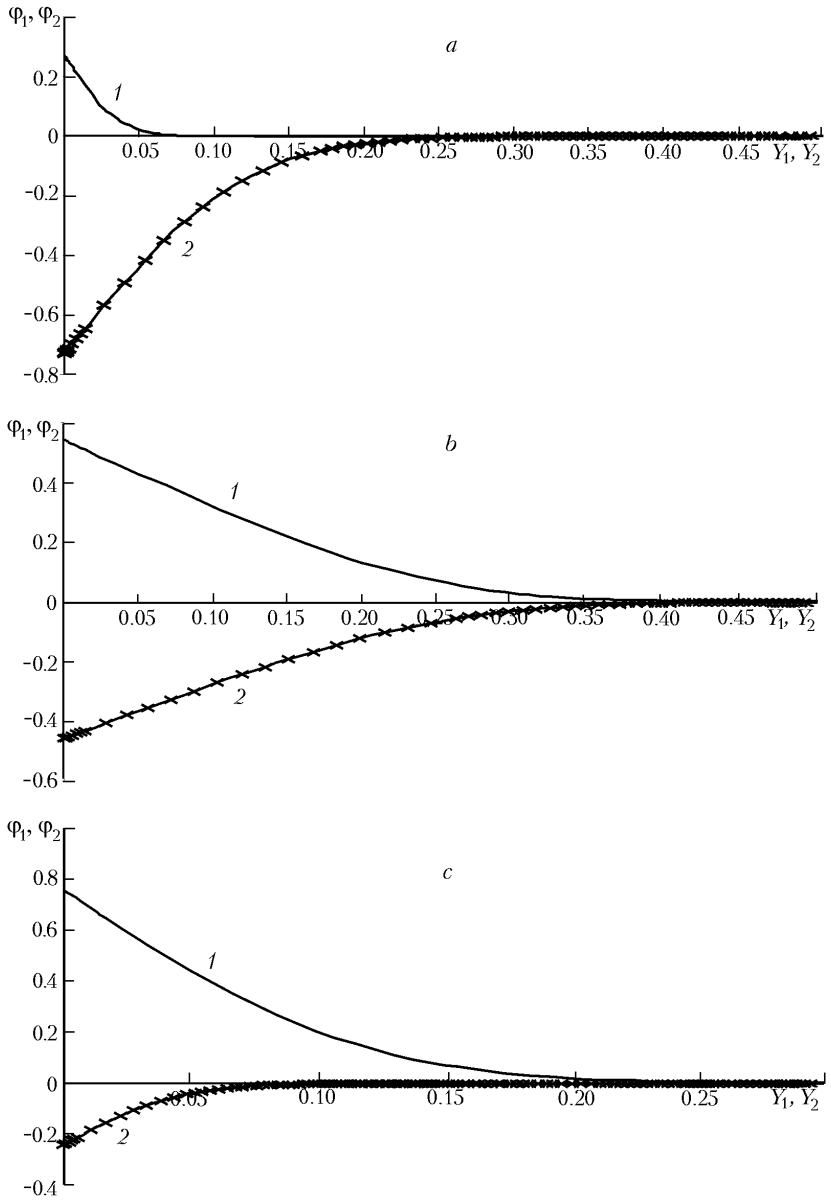

Fig. 2. Numerical results for φ_1 and φ_2 (curves 1 and 2, respectively) at θ_1 = 0.7, θ_2 = 1.2, θ_3 = 0.8029, and different values of X_1: X_1 = 0.1 (a), 0.5902 (b), and 0.9 (c).

The numerical results for the used values of the boundary conditions (α, β), the dimensionless mass flux at the interphase ($\varphi'_1(0)$, $\varphi'_2(0)$), and the boundary-layer thickness (η_i^{∞}, where $\varphi_i(\eta_i^{\infty}) \le 0.01$), are shown in Table 1. Dimensionless concentration distributions in the phases can be seen in Fig. 2.

Mass-Transfer Kinetics. The mass-transfer rate may be expressed by the mass-transfer coefficient and the average diffusion flux along the length of the interphase:

$$J_i = k_i \chi^{1-i} \left(c_1^{\infty} - \chi c_2^{\infty} \right) = \frac{D_i}{l} \int_0^l \left(\frac{\partial c_i}{\partial y} \right)_{y=0} dx \,, \tag{6}$$

which allows us to determine the Sherwood number:

$$\mathrm{Sh}_i = \frac{k_i l}{D_i} = \frac{\chi^{i-1}}{c_1^{\infty} - \chi c_2^{\infty}} \int_0^l \left(\frac{\partial c_i}{\partial y} \right)_{y=0} dx \,. \tag{7}$$

These equations can be presented in the following way with dimensionless variables and similarity parameters:

$$\mathrm{Sh}_i = -\sqrt{\mathrm{Re}_i} \int_0^1 \frac{\varphi_i'(0)}{\sqrt{X_i}} dX_i \,, \quad \mathrm{Re}_i = \frac{u_i^{\infty} l}{\nu_i} \,. \tag{8}$$

Comparison of Counter-Current and Co-Current Flows. The solutions obtained enable us to determine the mass-transfer rate using the average diffusion fluxes:

$$J_i = -\int_0^1 \frac{\varphi_i'(0)}{\sqrt{X_i}} dX_i \tag{9}$$

The average mass-flux values for the system in the case of counter-current flows at $\theta_1 = 0.7$, $\theta_2 = 1.2$, $\theta_3 = 7.56$, $\mathrm{Sc}_1 = 812$, and $\mathrm{Sc}_2 = 440$ are the following: $J_1 = 5.9093$, $J_2 = 4.7436$. To compare the mass-transfer rate for the counter-current and co-current flows, the system of differential equations should be solved with parameter values corresponding to the co-current flow as well. In the latter case, φ_i does not depend on X_1; thus, the mass-transfer rate can be presented as $J_i^* = -2\varphi_i'(0)$. For $\theta_1^* = -0.7$, $\theta_2^* = -1.2$, and $\theta_3^* = 7.56$ we obtain $J_1^* = 3.0446$ and $J_2^* = 23.0172$.

The comparison of these results shows that in phase 2 the mass-transfer rate of the counter-current flow is much below the rate in the case of co-current flow. In phase 1, however, these values are commensurable. The results obtained in [11] and in the present work allow us to determine the ratio between the mass-transfer rate and the corresponding energy dissipation in the cases of counter-current and co-current flows:

$$A_i = \frac{\mathrm{Sh}_i}{E_i} \,, \quad A_i^* = \frac{\mathrm{Sh}_i^*}{E_i^*} \,, \tag{10}$$

where E_i is the energy dissipation [1] (here $E_1 = 0.3488$, $E_2 = 0.3224$, $E_1^* = 0.0223$, and $E_2^* = 0.0283$). Comparative data for A_i in the cases of counter-current and co-current liquid—liquid flows are the following: $A_1 = 16.94$, $A_2 = 14.71$, $A_1^* = 136.5$, $A_2^* = 813.3$. They show higher efficiency of the co-current flow where the higher mass transfer rate is achieved at equal energy losses.

Conclusions. The numerical results obtained for the mass transfer between liquid–liquid counter-current flows show that the rate of interphase mass transfer J_i is limited by the diffusion resistance of phase 2 for small values of X_1, i.e., $J = J_2$. Otherwise, when X_1 is large, the diffusion resistances in the phases are commensurable. In counter-current flows, the velocity does not change direction in the concentration boundary layers near the interphase but changes it in both phases at different X_1 ($0 < X_1 < X_0$ in phase 1 and $X_0 < X_1 < 1$ in phase 2). The results obtained show that the co-current flow is more efficient energetically than the counter-current one due to lower energy losses at equal rates of mass transfer.

This work was completed with the financial support of the National Science Fund, Ministry of Education and Science, Republic of Bulgaria under Contract TH-1001/00.

NOTATION

c, concentration, kg/m^3; D, diffusivity, m^2/sec; E, dimensionless energy dissipation; J, interphase mass-transfer rate, kg/(m^2·sec); k, mass-transfer coefficient, m/sec; l, length, m; Re, Reynolds number; Sc, Schmidt number; Sh, Sherwood number; u and v, velocities in x and y directions, m/sec; x and y, longitudinal and transverse coordinates, m; μ, dynamic viscosity, kg/(m·sec); ν, kinematic viscosity, m^2/sec; χ, Henry number. Subscripts and superscripts: i = 1 and 2, liquids 1 and 2; ∞, potential flow; *, co-current flow.

REFERENCES

1. E. Horvath, E. Nagy, C. Boyadjiev, and J. Gyenis, Interphase mass transfer between liquid–liquid counter-current flows. I. Velocity distributions, *Inzh.-Fiz. Zh.*, **80**, No. 4, 80–85 (2007).
2. M. Doichinova and C. Boyadjiev, Opposite-current flows in gas–liquid boundary layers. II. Mass transfer kinetics, *Int. J. Heat Mass Transfer,* **43**, 2707–2710 (2000).
3. C. Boyadjiev and M. Doichinova, Opposite-current flows in gas–liquid boundary layers. I. Velocity distribution, *Int. J. Heat Mass Transfer,* **43**, 2701–2706 (2000).